行政院國家科學委員會補助專題研究計畫成果報告

※※※※※※※※※※※※※※※※※※※※※※※※※※

※ ※

※健康拜香之研發（一）： ※

※ 燃燒條件對拜香生成微粒與氣態污染物之影響 ※

※ ※

※※※※※※※※※※※※※※※※※※※※※※※※※※

計畫類別： X 個別型計畫 □整合型計畫

計畫編號： NSC 90－2320－B002－198

執行期間： 90 年 8 月 1 日至 91 年 7 月 31 日

計畫主持人：林嘉明

共同主持人：陳志傑

計畫參與人員：楊慈定

本成果報告包括以下應繳交之附件：

□赴國外出差或研習心得報告一份

□赴大陸地區出差或研習心得報告一份

□出席國際學術會議心得報告及發表之論文各一份

□國際合作研究計畫國外研究報告書一份

執行單位：國立台灣大學公共衛生學院

中 華 民 國 91 年 10 月 28 日

行政院國家科學委員會專題研究計畫成果報告

健康拜香之研發（一）：
燃燒條件對拜香生成微粒與氣態污染物之影響

CHARACTERIZATION OF AEROSOL EMISSION FROM SMOLDERING INCENSE

計畫編號：NSC 90－2320－B002－198
執行期限：90 年 8 月 1 日至 91 年 7 月 31 日

主持人：林嘉明　國立台灣大學環境衛生研究所
共同主持人：陳志傑　國立台灣大學職業醫學與工業衛生研究所
計畫參與人員：楊慈定　國立台灣大學環境衛生研究所

中文摘要

本研究探討拜香燃燒條件、熱值及原料對微粒及氣態污染物形成的影響。設定測試腔的流量率為 5 L/min, 改變氧氣的分率使拜香從燃燒到熄滅, 量測拜香表面的溫度, 同時使用直讀的儀器即時偵測測試腔內一氧化碳(CO)、二氧化碳(CO_2)、總有機蒸氣(VOCs)、粒狀物等的濃度以及粒狀物的粒徑分佈。另外, 使用卡計(oxygen bomb calorimeter)測量拜香的熱值。結果顯示, 當氧氣分率接近 45%時拜香開始悶燒, 低於 19%時則熄滅, 悶燒頂點的溫度隨氧氣分率之增加從 434℃提升到 637℃, 消耗的氧氣及拜香的燃燒率也隨箸增加, CO_2、CO、VOCs 等的釋放率也隨箸提高, 但 CO_2 及 VOC 的釋放因子減少, 而 CO 的釋放因子卻提高, 顯示拜香的悶燒結果是屬於熱分解。再者, 氣狀污染物的體積及數目之釋放率隨者氧氣分率增加, 但是體積的釋放因子隨燃燒點的溫度增高, 但數目濃度卻隨者溫度的升高而減少, 這種結果顯而易見的是因為凝結。在氧氣分率為 20%之下持續悶燒拜香時(如在寺廟燃燒), 釋放的氣狀及粒狀污染物的量最低。

關鍵詞：悶燒、熱分解、釋放因子、凝結

Abstract

The effects of combustion condition, heating value and the composition of incense on the characteristics of gases as well as particulates emitted from smoldering incense have been examined. In this work, the oxygen fraction at 5 L/min of airflow was adjusted from starting flame down to extinguishing, while the total airflow remained, as an incense stick smoldered in a test chamber. Carbon monoxide, carbon dioxide, VOCs, and particulates concentration as well as its size distributions in real-time were monitored. The temperature on the surface of the smoldering tip was measured using a homemade thermocouple, made of 79 μm nickel-aluminum and chrome wires. The heating value of an incense stick was measured using an oxygen bomb calorimeter.

Experimental results showed that the incense stick started flaming if the oxygen fraction was over close to 45%, and was extinguished if the oxygen fraction was lower than 19%. The temperature of the smoldering tip increased with an increasing oxygen fraction, ranging from 434 to 637℃. The oxygen consumed and the burning-rate increased with an increasing oxygen fraction. The CO_2, CO, and VOC emission rates also increased with oxygen fraction when the air flow was fixed at 5 L/min. The CO_2 and VOC emission factors decreased with an increasing

oxygen fraction, but the CO emission factor increased, indicating that incense smoldering is pyrolytic. Moreover, the aerosol number and volume emission rates increased with an increasing oxygen fraction. The emission factors of particle volume also increased with the temperature of the incense-burning point, but the particle number emission factor decreased, apparently because of coagulation. When continuously smoldering incense is required (such as in a temple), 20% O_2 produces the lowest a mount of gas and aerosol emissions for the incense tested in this work.

Keywords: smoldering, pyrolytic, emission factors, coagulation

Introduction

Burning incense sticks is a popular ritual in religious and folk worship. Despite the negative health effects of burning, many people can't stop to burn incense as a form of ritual worship. Studies have shown that incense burning cause health hazards. For instance, Hayakwa has reported contact dermatitis due to exposure to musk ambrette from incense (Hayakwa et al, 1987a; Hayakwa et al, 1987b). Smoke from burning incense has been related to lung cancer (MacLennan et al, 1977; Chen et al, 1990), childhood leukemia (Lowergard et al, 1987), brain tumors (Preston-Martin et al, 1982) and nasopharyngeal cancer (Chen et al, 1987; Yu et al, 1990), in a number of epidemiological studies. Cytotoxic studies have also indicated that the polycyclic aromatic hydrocarbons (PAHs) contained in incense smoke lead to mutagenic effects and sister chromatid exchange (Löfroth et al, 1991, 1997). In fact, Ames has identified this exact mutagenic effect of smoke from burning Chinese incense (Rasmussen, 1987).

Incense smoke is a complex mixture, containing mainly gas and a particulate phase. The gas phase consists of carbon monoxide, carbon dioxide, nitrogen oxides, formaldehyde, volatile organic compounds, aromatics and so forth. The particulate phase includes fine particulates in which are embedded such organic compounds as PAHs. Adverse health effects might be caused by the extremely high number of fine particulates and organic compounds, which when put together enhance the effects of each other and easily and deeply penetrate into the alveolar region of the respiratory system. Gaseous PAHs and aliphatic aldehydes also have a detrimental effect on health. Smoke has been proven to contain polycyclic aromatic hydrocarbons (Lin and Lee, 1998; Chang et al., 1997), aromatic aldehydes and aliphatic aldehydes (Lin and Wang, 1994).

Burning incense is the most common example of true smoldering combustion. Smoldering is a slow, low-temperature, flameless form of combustion, sustained by the heat evolved when oxygen directly attacks the surface of a condensed-phase fuel. Smoldering constitutes a serious fire and healthy hazard for two reasons. First, it typically converts substantially more fuel to toxic compounds than does flaming. Second, smoldering provides a pathway to flaming that can be initiated by heat sources much too weak to produce a flame directly (Ohlemiller).

Most of the past studies concerned with incense smoke focused on indoor air sampling and laboratory simulation in which combustion conditions were often not controlled. Few studies have explored the effects that combustion temperature, airflow, oxygen content, and other parameters have had on the yields of products due to the burning of incense. This study, therefore, seeks to elucidate the effects of combustion conditions on the yields of gaseous pollutants and particulates from burning incense sticks. Combustion conditions were controlled by altering the proportion of oxygen and nitrogen at a flow rate of 5 L/min.

Materials and Methods

Characteristics of Incense

A joss stick, named Chinese incense Yellow, was obtained from a local manufacturer. The joss stick consisted of incense powder and a bamboo stick. The incense powder was a mixture of three varieties of dried vegetation (Santalum album L., Machilus nanmu Hemsl, and Pine oleoresin). The Santalum and Pine oleoresin was sieved through a 60/60 mesh and Machilus was sieved through a 100/100 mesh. The elemental composition and heating value were analyzed at Taiwan Power Company's Laboratory. An elemental analyzer instrument measured carbon, hydrogen, and nitrogen. The heat value was measured by an oxygen bomb calorimeter.

Experimental System

Figure 1 schematically depicts the burning incense system. The system consisted of a gas mix chamber, a pollutant generation chamber in which incense was burnt, a test chamber, and two sampling gas dilution chamber. Oxygen and nitrogen from a cylinder, particles already cleaned by HEPA, were controlled by a mass flow controller and then led into the gas mix chamber to ensure complete mixing. Various proportions of oxygen to nitrogen in a 0.047L of mixture, at a flow rate of 5 L/min, entered the pollutant generation chamber. A joss stick of incense was ignited and inserted in a fine steel tube at the bottom of the pollutant generation chamber. The height of the burning tip of the incense was fixed by controlling the height of the fine steel. The gas and aerosol pollutants were generated and carried into the 4.7L test chamber. At 40 cm from the bottom of the test chamber, a 1/4-inch steel sampling tube was inserted 3.5cm from the wall of the test chamber, as a sampling probe to which various reading instruments were connected. Aerosol number concentration, aerosol size distribution, and VOCs in incense smoke were directly monitored without diluting the incense smoke. The concentrations of carbon monoxide, carbon dioxide, and oxygen, however, were measured after diluting the incense smoke because the concentrations exceeded the detection limits of the instruments. The study involved two small chambers, 0.42L for O_2, 1.4 L for CO_2 and CO, in which the incense smoke was diluted. The incense smoke passed through the sampling to the chambers and was mixed with pure nitrogen at a constant flow rate to reduce the pollutant's concentration to a range that could be detected.

After the tests were completed, the incense was extinguished by closing the oxygen and opening the nitrogen flows. Each round of testing took six minutes. Before and after burning, individual joss sticks were weighed to determine the net loss of mass, and thus the incense-burning rate could be calculated.

Monitoring Temperature of Tip of Burning Incense

The temperature on the surface of the incense-burning tip was continuously measured using a homemade K-type thermocouple of 79 μm nickel-aluminum and nickel-chrome wires. Data were recorded on a computer, using a data translation PICO TC-08 monitor (PICO Inc., St. Neots PE19 1QB, U.K.).

Monitoring Combustion Emissions

The concentrations of aerosol number and the size distribution of particles less than 1μm in diameter were measured using a TSI 3071 differential mobility analyzer (DMA) connected to a TSI 3022 condensation particle counter and operated in scanning mode by a personal computer. Carbon monoxide and carbon dioxide concentrations were monitored using Q-Trak™ Indoor Air Quality Monitor (Model 8550/8551, TSI Inc., St. Paul, MN, U.S.A.). The CO_2 sensor was of the non-dispersive infrared (NDIR) type, with a specified detection range of 0-5000 ppm, a response time of < 20 seconds, and a 1ppm resolution. A cylinder of pure nitrogen was used also to calibrate the zero of CO_2 concentration, and CO_2 standard concentration (4050 ppm) was used for span calibration. The CO sensor was of the electro-chemical type, with a range of detection of 0-500 ppm, a response time of < 60 seconds, and a resolution of 1ppm. A cylinder of pure nitrogen was used also to calibrate the zero of CO concentration, and CO standard concentration (395 ppm) was used for span calibration. Oxygen was monitored by a Mehrgas-Me β gerät multi-gas monitor (Multiwarn II, Dräger Sicherheitstechnik Gmbh Germany). The oxygen sensor was of the electro-chemical type, with a range of detection of 0-25%, and a resolution of 1%. The pure nitrogen served as zero calibration and the fresh air functioned for fresh air calibration.

VOCs were monitored using a MiniRAE 2000 Portable VOC Monitor (RAE SYSTEMS Inc., 1339 Moffett Park Drive, Sunnyvale, CA 94089). The VOC monitor with a Photo-ionization detector, could detect 0-10000 ppm. The response time and resolution were 2 seconds and 0.1~1ppm, respectively. The monitor was zero-calibrated using pure nitrogen and its responsive span was calibrated using a known isobutylene standard concentration (100 ppm).

Determining of Gas and Aerosol Emission Rate and Factor

According to a mass balance model, the gas and aerosol concentrations in the sampling test chamber are given by,

$$V \times \frac{dCi}{dt} = R \times E_F - Q \times Ci \quad (1)$$

where V (m^3) is the volume of the sampling test chamber; C_i (mg/m^3 or particles/cm^3) is the gas or aerosol concentration in the sampling test chamber at any time; R (g/hr) is the incense-burning rate; E_f (mg/g or particles/g) is the emission factor of each pollutant, and Q (5 L/min) is the air flow rate. This study neglects to note the appearance of pollutant deposition onto the surface of the sampling test chamber. After a short period of time passed over, each pollutant in the sampling chamber reached dynamic equilibrium. Since dCi/dt=0 in Eq. 1., the equation can thus be re-written as follows,

$$E_F = \frac{Q \times C}{R} \quad (2)$$

where C (mg/m^3 or particles/cm^3) is the equilibrium concentration of one pollutant in the sampling test chamber. For gaseous pollutants, the expression of concentration was converted from volume/volume units (ppm) at 25℃, 1 atm to mass/volume units (mg/m^3) based on the ideal gas law, PV=nRT, to apply properly Eqs. 1 and 2. Furthermore, molecular weights of VOCs were assumed to be 100 g. Consequently, the emission factor was calculated using Eq. 2. The emission rate was obtained by multiplying airflow rate by the pollutant concentration.

Results and Discussion

1. Elemental Composition and Heating Value of Incense

Table 1 shows the chemical composition and heating value of the incense, as determined by Taiwan Power Company's Laboratory. The carbon, hydrogen, nitrogen, ash, and water weight percentages were 43.59, 5.40, 0.61, 7.72 and 7.39 %, respectively. The heating value of incense was 3936 Kcal/Kg.

2. Incense Burning Rate and Quantity of Consumed Oxygen

Figure 2 presents the burning rate of a joss stick of yellow incense and the oxygen consumed for various oxygen fractions in 5 L/min gas. The combustion rate in 20, 25, 30, 35, and 40 % oxygen fractions of a single burning joss stick of yellow incense were 1.29, 1.64, 1.80, 2.30, and 2.71 g/hr, respectively, and 0.2, 1.9, 3.3, 4.2, and 5.7 % oxygen was consumed, respectively. The combustion law includes four important parameters: material, oxygen, temperature and chain-reaction. During combustion, consuming more material and oxygen releases more heat, and thus affects the surface temperature of the tip of the burning incense.

3. Time-Temperature Profiles On Surface Of An Incense Tip

The surface temperature on a burning tip of an incense stick was measured using a K-type thermocouple. At 12 cm from the bottom of the pollutant generation chamber, a K-type thermocouple was inserted 0.8 cm from the wall of the pollutant chamber. The char line of the burning-tip is defined as the dividing line between burning incense and incense unburned. When the burning incense was inserted into the chamber, the incense unburned which was at 0.5 cm from the char line of the burning incense, moved downward to touch the K-type thermocouple. The height of the incense of the burning tip declined as time passed, and the incense unburned which was at 0.2 cm from the char line of the burning incense move to touch the K-type thermocouple. As soon as the computer started to record the temperature from incense unburned to the top of the burning-tip.
Figure 3 illustrates the Time-temperature profiles on the surface of the incense tip under various oxygen fractions. Experimental results showed that while burning the incense under various combustion conditions, the temperature increases from the char line to the middle of the burning-tip. The temperature was highest in the middle of the burning tip, at which point very much heat was released because of incense-char oxidation. Subsequently, the temperature rapidly declined from the middle to the top of the burning-tip because of incense-char exhaust. Figure 4 plots the maximum surface temperature of a burning-incense tip.
The maximum temperature of the burning tip in 20, 25, 30, 35, and 40 % oxygen fractions in 5 L/min gas was 434, 482, 541, 590, and 637 ℃, respectively. The burning smoking incense was extinguished in close to 19 % oxygen and a flame was lit in approximately 45 % oxygen.

4. Particle Size Distribution

Figure 5 plots the number concentration and emission factors versus particle size under various combustion conditions. The results showed that all particles emitted during the steady burning of incense under various combustion conditions were smaller than 1.0 μm in diameter, and the vast majority had diameters within range of 0.1-0.3 μm. Burning incense generates a large majority of submicrometer particles, and therefore high levels of deposition in the alveolar region, with significant health implications. Furthermore, the emission factors of particles of size less than 300 nm decreased as oxygen fraction increases while those particles sized from 300 to 1000 nm increased with the oxygen fraction, apparently due to coagulation.
Figure 6 shows the particle count and volume median diameter from burning incense under various combustion conditions. The count median diameters of particles in 20, 25, 30, 35, and 40 % oxygen were 150, 163, 162, 174, and 180 nm, respectively. The volume median

diameters varied with 20, 25, 30, 35, and 40 % oxygen fractions were 285, 327, 336, 370 and 389 nm, respectively. The results show that the particle number and volume median diameters increased with oxygen fraction at an air flow rate of 5 L/min, apparently due to coagulation.

5. Gas Pollution Emission, Emission Rates and Factors

Table 2 presents the concentrations, emission rates, and emission factors of gas pollutants from burning incense. The concentrations of CO_2 emitted at 5 L/min of air flow rate in 20, 25, 30, 35, and 40 % oxygen fractions for burning a joss stick of incense were 1647, 1929, 2277, 2434, and 3041 ppm, respectively. The CO concentrations were 732, 1056, 1282, 1666, and 2341 ppm, respectively. The concentrations of VOCs were 39.4, 60.0, 64.5, 73.6, and 85 ppm, respectively.

The emission rate was the air flow rate multiplied by the pollutant concentration. The CO_2 emission rates in 20, 25, 30, 35, and 40 % oxygen fractions of 5 L/min from one burning joss stick of incense were 890, 1042, 1230, 1315, and 1642 mg/hr, respectively. The CO emission rates were 252, 363, 441, 573, and 805 mg/hr, respectively. The VOCs emission rates were 48.32, 73.66, 79.15, 90.38, and 104.4 mg/hr, respectively.

The CO_2 emission factors in 20, 25, 30, 35, and 40 % oxygen fractions of 5 L/min from one burning joss stick of incense were 685, 634, 680, 570, and 607 mg/g, respectively. The CO emission factors were 194, 221, 244, 248, and 297 mg/g. The VOCs emission factors were 41.75, 41.05, 40.71, 40.33, and 39.64 mg/g, respectively.

Figure 7 plots the concentrations of CO, CO_2, and VOCs, and corresponding emission factors from burning incense under various combustion conditions. The results show that the concentrations of CO_2, CO, and VOCs increased linearly with oxygen fractions at 5 L/min of air. Both CO_2 and VOC emission factors declined as oxygen fraction increased, but CO emission factors did not. The CO_2 emission factors linearly declined as the surface temperature of the burning tip increased, indicating that the burning of incense might be pyrolytic.

6. Aerosol Emission, Emission Rates and Factors

Table 3 lists particle concentrations, emission rates and emission factors during the burning of incense.

The particle number concentrations in 20, 25, 30, 35, and 40 % oxygen from burning one joss stick of incense were 1.08×10^7, 1.34×10^7, 1.49×10^7, 1.51×10^7, and 1.74×10^7 #/cm^3, respectively. The particle volume concentrations were 6.95×10^{13}, 1.22×10^{14}, 1.39×10^{14}, 1.86×10^{14} and 2.44×10^{14} nm^3/cm^3, respectively. The particle number emission rates were 3.23×10^{12}, 4.02×10^{12}, 4.48×10^{12}, 4.53×10^{12}, and 5.22×10^{12} #/hr, respectively. The particle volume emission rates were 2.09×10^{19}, 3.65×10^{19}, 4.17×10^{19}, 5.57×10^{19} and 7.31×10^{19} nm^3/cm^3, respectively. The particle number emission factors were 2.81×10^{12}, 2.24×10^{12}, 2.30×10^{12}, 2.02×10^{12}, and 1.99×10^{12} #/g, respectively. The particle volume emission factors were 1.81×10^{19}, 2.03×10^{19}, 2.14×10^{19}, 2.49×10^{19} and 2.78×10^{19} nm^3/cm^3, respectively.

Figure 8 presents the particle number, volume concentrations, and emission factors from burning incense under various combustion conditions. The aerosol number and volume concentrations increased linearly with the oxygen fraction in 5 L/min of air. The particle volume emission factors increased linearly with the maximum temperature of the incense-burning tip but the particle number emission factors declined linearly, apparently due to coagulation. According to the results for gas and aerosol emission rates, where continuous smoldering incense is necessary (such as in a temple), 20% O_2 produces the lowest gas and aerosol emissions for the incense tested in this work.

7. Combustion Efficiency

Figure 9 reveals the combustion efficiency index of burning incense under different combustion condition. This study used (CO) / (CO_2+CO) as a combustion efficiency index. The combustion efficiency index increased linearly with an oxygen fraction between 20%~40%. The results indicate that the incenses burned more incompletely with oxygen fractions between 20%~40%.

8. Kinetics of Evolution of Burning Rate and Products of Burning-Incense

Figure 10 shows Arrhenius plots of individual burning rates, gas and particle emission rates versus $(1/T_{max})*1000$. The results show that logarithms of individual CO_2, CO, VOCs, (CO)/(CO+CO_2), particle number and volume emission rates versus $(1/T_{max})*1000$ are linearly related.

Conclusions

1. The incense stick started flaming when the oxygen portion exceeded approximately 45% and was extinguished when the oxygen was lower than 19%. The maximum temperature of the burning-tip increased with the oxygen fraction, ranging from 433 to 637℃.
2. The temperature of the burning-tip at which incense burns and oxygen is consumed increased with the oxygen fraction. A higher fraction of oxygen was found to cause the incense stick to burn faster, as expected.
3. The CO_2, CO, and VOC emission rates linearly increase with oxygen fractions at 5 L/min. The CO_2 and VOC emission factors linearly decline as the oxygen fraction increases but the CO emission does not. The CO_2 and CO emission rates and factors indicate that incense may burn pyrolytically.
4. The aerosol number and volume emission rates linearly increase with oxygen fraction. The particle volume emission factors linearly increase with the maximum temperature at which the tip of the incense burns, but the particle number emission factor decreases, apparently due to coagulation.
5. According to gas and aerosol emission rates, when continuously smoldering incense is required (such as in a temple), then the best burning-incense condition is in 20% oxygen at 5 L/min, as the gaseous and particle emissions are lowest for the incense tested in this work.

Acknowledgement

The authors would like to thank the National Science Council of the Republic of China for financially supporting this research under Contract No. NSC-90-2320-B-002-198.

References

Hayakawa, R., K. Mataunaga, and Y. Arima, "Airborne pigmented contact dermatitis due to musk ambrette in incense," Contact Dermatitis, 16, pp.96-98 (1987)

Hayakawa, R., K. Mataunaga, and Y. Arima, "Depigmented contact dermatitis due to incense," Contact Dermatitis, 16, pp.272-274 (1987)

Lowengard, R.A., J.M. Peters, C. Cinioni, J. Buckley, L. Bernstein, S. Preston-Martin, and R. Edward, "Childhood leukemia and parents' occupation and home exposure," JNCI., 79, pp.39-45 (1987)

Preston-Martin, S., MC. Yu, B. Benton, and BE. Henderson, "N-Nitroso compounds and childhood brain tumors: A case-control study," Can Res., 42, pp.5240-5245 (1982)

Chen, C.J., Y.F. Wang, T. Shied, J.Y. Chen, and M.Y. Liu "Multifactorial etiology of nasopharyngeal carcinoma," Head and Nect Oncology Research Conference, 10-12, pp. 469-476 (1987)

Yu, M.C., D.H. Garabrant, T.B. Huang, and B.E. Henderson "Occupational and other nondietary risk factors for nasopharyngeal carcinoma in Guanzhou," China Int J Cancer, 45, pp.1033-1039 (1990)

Maclennan, R., J.D. Costa, N.E. Day, C.H. Law, Y.K. Ng, K. Shanmugaratnam, " Risk factors for lung cancer in Singapore Chinese, A population with high female incidence rates," Int J Cancer., 20, pp. 854-860 （1977）

Chen, C.J., H. Y. Wu, Y.C. Chuang, A. S. Chang, K.T. Luh, H.H. Chao, K.Y. Chen, S.G. Chen, G.M. Lai, H.H. Huang, and Lee H.H. "Epidemiologic characteristics and multiple risk factors of lung cancer in Taiwan," Anticancer Research, 10(4), pp. 971-976 (1990)

Lofroth, G., C. Stensman, and B.S. Margareta, "Indoor sources of mutagenic aerosol particulate matter: smoking, cooking and incense burning," Mutation Research.,261, pp.21-28 （1991）

Rasmussen, R. E. " Mutagenic activity of incense smoke in Salmonella typhimurium," Bull Environ Contam Toxicol., 38, pp. 827-833 （1987）

Lin, J.M. and C.S. Tang, "Characterization and aldehyde content of particulates in Chinese incense smoke," Bull. Environ. Contam. Toxicol., 53, pp. 895-901 （1994）

Lin, J.M. and J.K. Lee, "Vaporous and particulate-bound polycyclic aromatic hydrocarbons in Chinese incense smoke," Toxicological and Environmental Chemistry, 67, pp. 105-113 （1998）

Lin, J.M. and L.H. Wang, "Gaseous aliphatic aldehydes in Chinese incense smoke," Bull. Environ. Contam. Toxicol., 58, pp. 394-401 （1994）

Ohlemiller, T.J, "Smoldering combustion," SPFE Handbook of Fire. Ed. DiNenno, P.M.,et al. 2 eds, pp. 171-179.

Table 1 Chemical compositions and heating value of incense

	incense
C	43.59%
H	5.40%
N	0.61%
Ash	7.72%
Water	7.39%
Heating Value	3936 Kcal/Kg

Table 2 Gas Pollutants emission concentration, rate and factors while burning incense

	Fraction of Oxygen (%	20	25	30	35	40
Emission	CO_2 (ppm)	1647	1929	2277	2434	3041
	CO (ppm)	732	1056	1282	1666	2341
	VOC (ppm)	39.4	60.0	64.5	73.6	85.0
Emission Rate	CO_2 (mg/hr)	890	1042	1230	1315	1642
	CO (mg/hr)	252	363	441	573	805
	VOC (mg/hr)	48.32	73.66	79.15	90.38	104.4
Emission Factor	CO_2 (mg/g)	685	634	680	570	607
	CO (mg/g)	194	221	244	248	297
	VOC (mg/g)	41.75	41.05	40.71	40.33	39.64

Table 3 Aerosol emission concentration, rate and factors while burning incense

	Fraction of Oxygen (%	20	25	30	35	40
Emission	number (#/cm^3)	1.08E+07	1.34E+07	1.49E+07	1.51E+07	1.74E+07
	volume (nm^3/cm^3)	6.95E+13	1.22E+14	1.39E+14	1.86E+14	2.44E+14
Emission Rate	number (#/hr)	3.23E+12	4.02E+12	4.48E+12	4.53E+12	5.22E+12
	volume (nm^3/hr)	2.09E+19	3.65E+19	4.17E+19	5.57E+19	7.31E+19
Emission Factor	number (#/g)	2.81E+12	2.24E+12	2.30E+12	2.02E+12	1.99E+12
	volume (nm^3/g)	1.81E+19	2.03E+19	2.14E+19	2.49E+19	2.78E+19

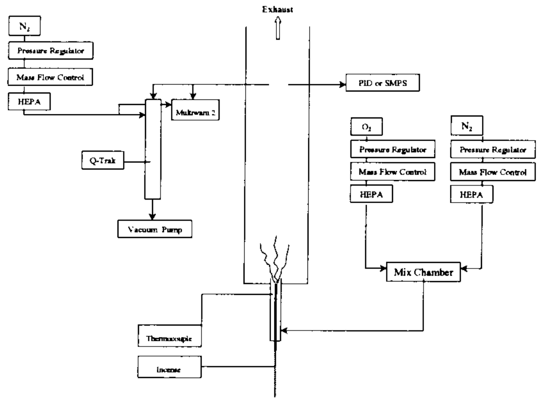

FIGURE 1 Schematic diagram of incense combustion system

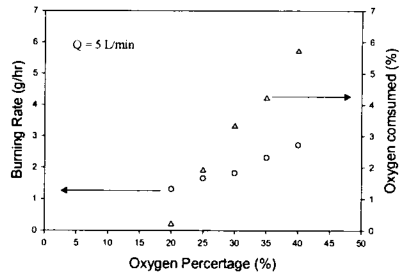

FIGURE 2 Burning rate and oxygen consumed under various oxygen fractions

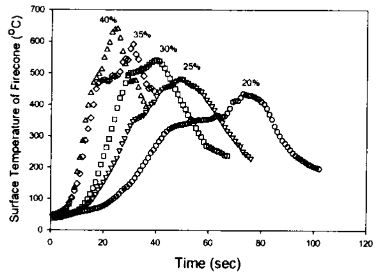

FIGURE 3 Time-temperature profiles on the surface of the incense tip under various oxygen fractions

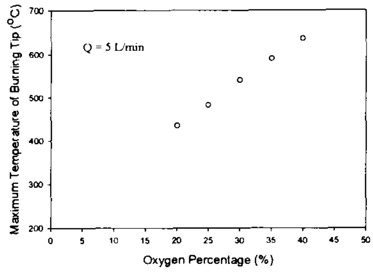

FIGURE 4 Maximum surface temperature of incense tip under various oxygen fractions

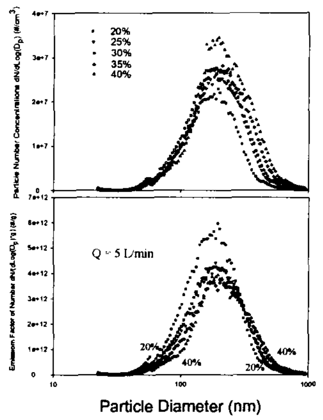

FIGURE 5 Aerosol number concentrations and emission factors versus particle size from burning incense under various combustion conditions

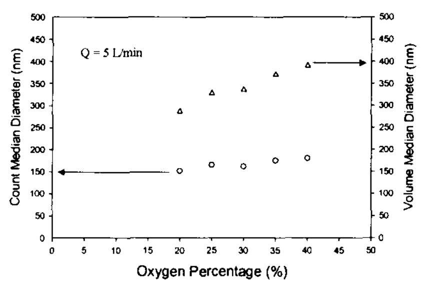

FIGURE 6 Count and volume median diameter of single incense stick under various oxygen fractions

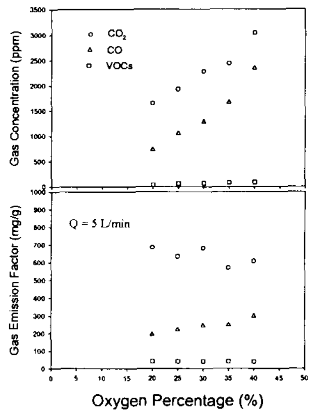

FIGURE 7 CO_2, CO, and VOCs emission concentrations, and corresponding emission factors from burning incense under various oxygen fractions

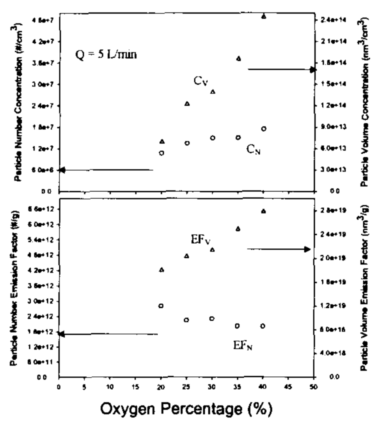

FIGURE 8 Aerosol number, volume emission and emission factors from burning incense under various oxygen fractions

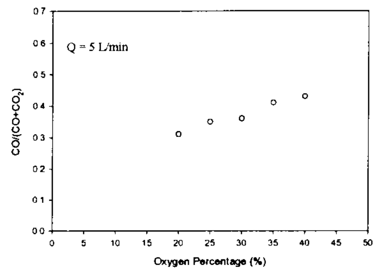

FIGURE 9 Combustion efficiency index from one burning joss stick of yellow incense under various oxygen fractions at 5 L/min

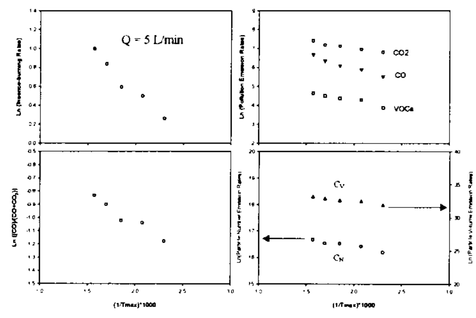

FIGURE 10 Logarithms of emitted yields of individual CO_2, CO, VOCs, aerosol and $((CO)/(CO+CO_2))$ as against function of (1/Tmax)*1000